MycoKeys 125: 347–368 (2025)
DOI: 10.3897/mycokeys.125.174645

Research Article

Morphological and phylogenetic analyses reveal three new species associated with *Pueraria* from Xizang Autonomous Region, China

Gui-Li Zhao[1,2], Yong-Zhong Lu[2,3], Xing-Juan Xiao[3], Ying Liu[1], Qiang Chen[1], Ning-Guo Liu[2,3]

1 *School of Chemical Engineering, Guizhou Institute of Technology, Guiyang 550025, China*
2 *Guizhou Key Laboratory of Agricultural Microbiology, Guizhou Academy of Agricultural Sciences, Guiyang 550009, China*
3 *School of Food and Pharmaceutical Engineering, Guizhou Institute of Technology, Guiyang 550025, China*
Corresponding author: Ning-Guo Liu (ningguol@git.edu.cn)

Abstract

During a survey of microfungi associated with *Pueraria* in the Xizang Autonomous Region, China, three saprobic taxa were isolated from the dead vines of *Pueraria* sp. Based on morphological characteristics and multi-gene phylogenetic analyses, the three taxa are identified as new species, viz., *Hermatomyces nyingchiensis*, *H. xizangensis*, and *Rhytidhysteron xizangense*. Morphological descriptions and illustrations of these new collections, along with a synopsis of *Hermatomyces* species, are provided.

Key words: 3 new taxa, Dothideomycetes, phylogeny, *Pueraria*-associated microfungi, taxonomy

OPEN ACCESS

Academic editor:
Samantha C. Karunarathna
Received: 12 October 2025
Accepted: 14 November 2025
Published: 27 November 2025

Citation: Zhao G-L, Lu Y-Z, Xiao X-J, Liu Y, Chen Q, Liu N-G (2025) Morphological and phylogenetic analyses reveal three new species associated with *Pueraria* from Xizang Autonomous Region, China. MycoKeys 125: 347–368. https://doi.org/10.3897/mycokeys.125.174645

Copyright: © Gui-Li Zhao et al.
This is an open access article distributed under terms of the Creative Commons Attribution License (Attribution 4.0 International – CC BY 4.0).

Introduction

Species of *Pueraria* (Leguminosae) are widely distributed across Asia, North America, and South America (Wang et al. 2020). They exhibit strong colonization ability and ecological adaptability, enabling them to survive and thrive even in post-mining environments, thereby contributing to the restoration of degraded lands (Singhal 2009). Members of *Pueraria* contain numerous compounds, including puerarin, isoflavones, flavones, flavonols, coumestrols, and other related phytochemicals (Chen et al. 2018; Wang et al. 2020; Chen et al. 2021; Wang et al. 2021; Zhang et al. 2021). These compounds possess diverse pharmacological activities, including anti-alcoholism (Xiong et al. 2010), antioxidant (Zhang et al. 2017; Son et al. 2019), hepatoprotective (Xu et al. 2013), and antidiabetic effects (Shukla et al. 2017; Wang et al. 2017; Sun et al. 2019). Although previous studies have investigated the arbuscular mycorrhizal fungi associated with *Pueraria* (Guo et al. 2022), research on saprophytic fungi related to *Pueraria* remains limited. In this study, we aim to explore the diversity of fungi associated with *Pueraria*, with a focus on saprobic fungal communities.

Hermatomyces was established by Spegazzini (1910), with *H. tucumanensis* as the type species. It was initially placed within Lophiotremataceae (Doilom et al. 2016; Tibpromma et al. 2017). However, Hashimoto et al. (2017) excluded

Hermatomyces from Lophiotremataceae and reinstated Hermatomycetaceae based on molecular evidence. Most species of *Hermatomyces* are known from their asexual morph, characterized by sporodochial conidiomata and dimorphic conidia (cylindrical and lenticular) (Doilom et al. 2016; Tibpromma et al. 2017; Koukol et al. 2018; Ren et al. 2021; Zhang et al. 2023; Liu et al. 2024). The sexual morph was recently described and is characterized by dark brown to black ascomata with a central ostiole, 8-spored, bitunicate asci, and hyaline, broadly fusiform, 1-septate ascospores (de Silva et al. 2022).

Rhytidhysteron was originally established by Spegazzini (1881) and was historically placed within Patellariaceae (Bezerra and Kimbrough 1982). However, molecular evidence provided by Boehm et al. (2009) demonstrated that *Rhytidhysteron* is not phylogenetically related to Patellariaceae but rather belongs to Hysteriaceae. Currently, 44 records of *Rhytidhysteron* are listed in Index Fungorum (http://www.indexfungorum.org, accessed 13 October 2025). Most species are known from their sexual morphs, whereas only four species have been recognized from their asexual morphs, which produce two types of conidia: aposphaeria-like and diplodia-like (Samuels and Müller 1979; Thambugala et al. 2016; Ren et al. 2022). The sexual morph of *Rhytidhysteron* is characterized by prominent, sizable, navicular ascomata, typically with perpendicular striations along the margins (Thambugala et al. 2016; de Silva et al. 2020; Wanasinghe et al. 2021; Ren et al. 2022; Du et al. 2023). The ascospores are pigmented, septate, and muriform to sub-muriform (Thambugala et al. 2016; Ren et al. 2022). Species within this genus play essential ecological roles, functioning as saprobes, endophytes, and mild pathogens on woody substrates in terrestrial and aquatic environments. Occasionally, some species have also been reported as human pathogens (Thambugala et al. 2016; Soto-Medina and Lücking 2017; de Silva et al. 2020; Wanasinghe et al. 2021; Ren et al. 2022; Du et al. 2023).

We aim to carry out a survey investigating fungal diversity associated with *Pueraria* sp. from the Xizang Autonomous Region, China. During this survey, three taxa were obtained. Based on morphological characterization, illustrations, and multi-gene phylogenetic analyses, *Hermatomyces nyingchiensis* sp. nov., *H. xizangensis* sp. nov., and *Rhytidhysteron xizangense* sp. nov. are described herein.

Materials and methods

Specimen collection, examination, and isolation

Specimens were collected from dead vines of *Pueraria* species in the Xizang Autonomous Region, China, and packed into plastic bags with recorded details such as collection date, locality, and host. The specimens were transported to the laboratory for examination and isolation. Morphological examination and single-spore isolations followed the methodologies described by Senanayake et al. (2020). Germinated spores were carefully transferred onto fresh potato dextrose agar (PDA) medium and incubated at room temperature. During this period, morphological characteristics of the colonies, such as color, form, and texture, were observed and recorded. Fungal colonies growing on the substrate were examined using Nikon SMZ 745 and SMZ 800N (Nikon, Tokyo, Japan) dissecting microscopes. Detailed microscopic observations and image capture were performed with a Nikon ECLIPSE microscope equipped with a Nikon DS-Ri2 digital camera.

Pure cultures were deposited in the Guizhou Culture Collection (GZCC), Guiyang, China, and dried specimens were preserved in the Herbarium of Cryptogams, Kunming Institute of Botany, Academia Sinica (HAKS), Kunming, China. The new species were registered in Fungal Names (https://nmdc.cn/fungalnames/).

DNA extraction, PCR amplification, and sequencing

Molecular analyses were conducted following the protocols outlined by Dissanayake et al. (2020). Genomic DNA was extracted from freshly grown mycelia on PDA plates using the Ezup Column Fungi Genomic DNA Purification Kit (Sangon Biotech, Shanghai, China), according to the manufacturer's instructions. Amplification of the large subunit ribosomal RNA region (LSU) was performed with the primers LR0R and LR5 (Vilgalys and Hester 1990); the internal transcribed spacer (ITS) region with ITS5 and ITS4 (White et al. 1990); the translation elongation factor 1-alpha (*tef*1-α) with EF1-983F and EF1-2218R (Rehner and Buckley 2005); the RNA polymerase II second largest subunit (*rpb*2) with fRPB2-5F and fRPB2-7cR (Liu et al. 1999); the β-tubulin (*tub*2) with primers T1 and T22 (O'Donnell and Cigelnik 1997); and the small subunit ribosomal RNA region (SSU) with NS1 and NS4 (White et al. 1990). Polymerase chain reaction (PCR) was conducted in a 25 µl volume containing 21 µl of 1.1 × T3 Super PCR Mix (Qingke Biotech, Chongqing, China), 1 µl of each primer, and 2 µl of DNA template. PCR amplification was initiated by denaturation at 98 °C for 2 min, followed by 40 cycles of 98 °C for 10 s, annealing at 55 °C for 1 min, and extension at 72 °C for 30 s. A final extension was performed at 72 °C for 2 min. Purification and sequencing of the PCR products were conducted by Tsingke Biotechnology Co., Ltd. (Beijing, China).

Phylogenetic analyses

All newly generated sequences were checked using BioEdit v. 7.0.5.3 to assess sequence quality. Forward and reverse sequences were assembled using SeqMan v. 7.0.0 (DNASTAR, Madison, WI, USA) (Clewley 1995). Sequences used in phylogenetic analyses were obtained from GenBank (http://blast.ncbi.nlm.nih.gov/) based on BLASTn search results and relevant literature (Doilom et al. 2016; Tibpromma et al. 2016, 2017; Soto-Medina and Lücking 2017; Koukol et al. 2018; de Silva et al. 2020; Ren et al. 2021; Du et al. 2023; Zhang et al. 2023). Multiple sequence alignments were carried out using the online MAFFT version 7 (https://mafft.cbrc.jp/alignment/server/) (Katoh and Standley 2013). Single alignment trimming was conducted using trimAl v. 1.2 (Capella-Gutiérrez et al. 2009) with the gappyout option. Maximum Likelihood (ML) and Bayesian Inference (BI) analyses were conducted online via the CIPRES Science Gateway platform (https://www.phylo.org/portal2/home.action). The ML trees were constructed using RAxML-HPC v. 8 on XSEDE (version 8.2.12), employing the GTRGAMMA model and 1,000 bootstrap replicates. Posterior probabilities (PP) were estimated through BI analyses using the Markov chain Monte Carlo (MCMC) algorithm implemented in MrBayes on XSEDE (version 3.2.7a) (Ronquist et al. 2012). In *Hermatomyces*, the optimal models applied were: TNe+R2 for LSU, TIM2e+I+G4 for ITS, TN+F+R3 for *tef*1-α, TNe+G4 for *rpb*2, and K2P+I for *tub*2. In *Rhytidhysteron*, the optimal models were: TN+F+R2 for LSU, K2P+G4 for ITS, K2P+I for SSU, and TIM2e+I+G4 for *tef*1-α. Markov chains were run for

50,000,000 generations, with trees sampled every 100 generations. Phylogenetic trees were visualized using FigTree v. 1.4.4, and final figure layouts were edited using Adobe Illustrator CC 2019 (version 23.1.0; Adobe Systems, San Jose, CA, USA). The sequences generated in this study were submitted to GenBank, and their accession numbers are listed in Tables 1, 2.

Table 1. Strains and sequence accession numbers included for analysis of *Hermatomyces*. The newly generated sequences are in bold. "T" indicates the type strains. NA indicates sequence unavailability.

Fungal Species	Strain numbers	Conidia type	Country	LSU	ITS	*tef*1-α	*rpb*2	*tub*2	References
Anteaglonium parvulum	MFLUCC 14-0823	-	Thailand	KU922917	NA	KU922922	NA	NA	Jayasiri et al. (2016)
A. thailandicum	MFLUCC 14-0816	-	Thailand	KU922909	NA	KU922920	NA	NA	Jayasiri et al. (2016)
Hermatomyces amphisporus	CBS 146613	2	USA	LR812662	LR812662	LR812657	LR812668	LR812673	Delgado et al. (2020)
H. amphisporus	CBS 146614	2	USA	LR812666	LR812666	LR812660	LR812671	LR812676	Delgado et al. (2020)
H. anomianthi	MFLUCC 21-0202^{T}	1 (Sexual)	Thailand	OK655817	OL413437	OM117546	NA	NA	de Silva et al. (2022)
H. bauhiniae	MFLUCC 16-0395^{T}	2	Thailand	MK443378	MK443382	MK443384	MK443386	NA	Hyde et al. (2019)
H. bifurcatus	CCF 5899	2	Panama	NA	LS398262	LS398416	LS398343	LS398441	Koukol et al. (2018)
H. bifurcatus	CCF 5900^{T}	2	Panama	NA	LS398263	LS398417	LS398344	LS398442	Koukol et al. (2018)
H. clematidis	MFLUCC 17-2085^{T}	2	Thailand	MT214556	MT310603	MT394735	MT394684	NA	Phukhamsakda et al. (2020)
H. constrictus	CCF 5904^{T}	2	Panama	LS398264	LS398264	LS398418	LS398345	NA	Koukol et al. (2018)
H. griseomarginatus	PRC 7201	1	Benin	NA	PP779919	PP840395	PP840388	NA	Koukol et al. (2025)
H. griseomarginatus	PRC 7203^{T}	1	Benin	NA	PP779918	PP840396	PP840389	NA	Koukol et al. (2025)
H. hainanensis	GZCC 23-0592^{T}	2	China	OR091329	OR098708	NA	NA	NA	Zhang et al. (2023)
H. hongheensis	KUNCC 23-13503^{T}	1	China	PP189897	PQ340461	PQ456948	PQ348601	NA	Shen et al. (2024)
H. hongheensis	KUNCC 23-14231^{T}	1	China	PP189898	PQ340462	PQ456949	NA	NA	Shen et al. (2024)
H. indicus (*H. thailandicus*)	MFLUCC 14-1145	2	Thailand	KU764694	KU144922	KU872756	KU712490	NA	Doilom et al. (2016)
H. indicus (*H. thailandicus*)	MFLUCC 14-1143^{T}	2	Thailand	KU764692	KU144920	KU872754	KU712488	NA	Doilom et al. (2016)
H. iriomotensis	KH 361^{T}	2	Japan	LC194367	LC194483	LC194394	LC194449	NA	Hashimoto et al. (2017)
H. jinghaensis	HKAS 112167^{T}	2	China	MW989519	MW989495	MZ042642	NA	NA	Ren et al. (2021)
H. krabiensis	MFLUCC 16-0249^{T}	2	Thailand	KX525742	KX525750	KX525758	KX525754	NA	Tibpromma et al. (2016)
H. krabiensis (*H. chiangmaiensis*)	MFLUCC 16-2817	2	Thailand	KY559394	NA	NA	NA	NA	Tibpromma et al. (2016)
H. maharashtraense	NFCCI 4879^{T}	1	India	MZ099917	MZ147016	MZ130659	MZ130660	NA	Wijayawardene et al. (2021)
H. maharashtraense	NFCCI 4880	1	India	MZ147042	MZ147019	MZ130661	MZ130662	NA	Wijayawardene et al. (2021)
H. megasporus	CCF 5897	2	Panama	NA	LS398265	LS398419	LS398346	LS398444	Koukol et al. (2018)
H. megasporus	CCF 5898^{T}	2	Panama	NA	LS398266	LS398420	NA	LS398445	Koukol et al. (2018)
H. nabanheensis	KUMCC 16-0149^{T}	2	China	KY766059	KY766058	KY766061	NA	NA	Hyde et al. (2017)
H. nujiangensis	HKAS 144367	1	China	PV264903	PV264897	PV261935	PV261929	NA	Yang et al. (2025)
H. nujiangensis	HKAS 144368	1	China	PV264904	PV264898	PV261936	PV261930	NA	Yang et al. (2025)
H. nyingchiensis	**GZCC 25-0849^{T}**	**2**	**China**	**PX413305**	**PX561052**	**PX436849**	**PX436845**	**PX436853**	**This study**
H. pyriformis	CGMCC 3.27462^{T}	1	China	PP491962	PP491964	PP505452	PP505454	NA	Du et al. (2024)
H. pyriformis	UESTCC 23.0441	1	China	PP491963	PP491965	PP505453	PP505455	NA	Du et al. (2024)
H. reticulatus	CCF 5893	1	Panama	LS398267	LS398267	LS398421	LS398347	LS398446	Koukol et al. (2018)
H. reticulatus (*H. subiculosus*)	MFLUCC 15-0843	1	Thailand	KX259523	KX259521	KX259527	KX259529	NA	Hyde et al. (2016)
H. sphaericoides	CCF 5908^{T}	1	Panama	LS398273	LS398273	LS398427	LS398352	LS398450	Koukol et al. (2018)

Fungal Species	Strain numbers	Conidia type	Country	LSU	ITS	*tef*1-α	*rpb*2	*tub*2	References
H. sphaericoides	CCF 5895	1	Panama	LS398270	LS398270	LS398424	LS398350	LS398447	Koukol et al. (2018)
H. sphaericus	PMA 116080	1	Panama	LS398281	LS398281	LS398431	LS398356	LS398454	Koukol et al. (2018)
H. sphaericus	PRC 4104	1	Panama	NA	LS398278	LS398430	LS398355	LS398453	Koukol et al. (2018)
H. sphaericus	MFLUCC 21-0036	1	Thailand	MW989516	MW989492	MZ042639	MZ042636	MZ042643	Ren et al. (2021)
H. sphaericus (*H. biconisporus*)	KUMCC 17-0183	2	China	MH260296	MH275063	MH412771	MH412755	NA	Tibpromma et al. (2018)
H. sphaericus (*H. chromolaenae*)	MFLUCC 16-2818	1	Thailand	KY559393	NA	NA	NA	NA	Tibpromma et al. (2017)
H. sphaericus (*H. pandanicola*)	MFLUCC 16-0251	2	Thailand	KX525743	KX525751	KX525759	KX525755	NA	Tibpromma et al. (2016)
H. sphaericus (*H. saikhuensis*)	MFLUCC 16-0266	1	Thailand	KX525740	KX525748	KX525756	KX525752	NA	Tibpromma et al. (2016)
H. sphaericus (*H. tectonae*)	MFLUCC 14-1141	2	Thailand	KU764696	KU144918	KU872758	NA	NA	Doilom et al. (2016)
H. sphaericus (*H. tectonae*)	MFLUCC 14-1140	2	Thailand	KU764695	KU144917	KU872757	KU712486	NA	Doilom et al. (2016)
H. trangensis	BCC 80742	1	Thailand	KY790601	KY790599	KY790607	KY790605	NA	Nuankaew et al. (2019)
H. trangensis	BCC 80741^{T}	1	Thailand	KY790600	KY790598	KY790606	KY790604	NA	Nuankaew et al. (2019)
H. tucumanensis	CCF 5912	2	Panama	LS398288	LS398288	LS398435	LS398360	LS398458	Koukol et al. (2018)
H. tucumanensis	CCF 5915	2	Panama	LS398290	LS398290	LS398437	LS398362	NA	Koukol et al. (2018)
H. turbinatus	MFLUCC 21-0038^{T}	2	Thailand	MW989518	MW989494	MZ042641	MZ042638	MZ042645	Ren et al. (2021)
H. verrucosus	CCF 5903^{T}	1	Panama	LS398292	LS398292	LS398439	LS398364	LS398462	Koukol et al. (2018)
H. verrucosus	CCF 5892	1	Panama	LS398291	LS398291	LS398438	LS398363	LS398461	Koukol et al. (2018)
H. xizangensis	**GZCC 25-0850^{T}**	**1**	**China**	**PX413303**	**PX561050**	**PX436847**	**PX436843**	**NA**	**This study**
H. xizangensis	**GZCC 25-0853**	**1**	**China**	**PX413304**	**PX561051**	**PX436848**	**PX436844**	**NA**	**This study**

Table 2. Strains and sequence accession numbers included for analysis of *Rhytidhysteron*. The newly generated sequences are in bold. "T" indicates the type strains. NA indicates sequence unavailability.

Fungal Species	Strain numbers	LSU	ITS	*tef*1-α	SSU
Gloniopsis calami	MFLUCC 15-0739	NG_059715	KX669036	KX671965	KX669034
G. praelonga	CBS 112415	FJ161173	NA	FJ161090	FJ161134
Rhytidhysteron bannaense	KUMCC 21-0483	OP526409	OP526399	OP572200	OP526395
R. bannaense	KUMCC 21-0482^{T}	OP526408	OP526398	OP572199	OP526395
R. bruguierae	KUMCC 21-0484	OP482285	OP494090	OP572207	OP482277
R. bruguierae	MFLU 18-0571T	MN017833	NA	MN077056	MN017901
R. bruguierae	MFLUCC 17-1515	MN632452	MN632457	MN635661	MN632463
R. bruguierae	MFLUCC 17-1511	MN632454	MN632459	NA	MN632465
R. bruguierae	MFLUCC 17-1502	MN632453	MN632458	MN635662	MN632464
R. bruguierae	MFLUCC 17-1509	MN632455	MN632460	NA	MN632466
R. camporesii	KUMCC 21-0488	OP482286	OP494091	OP572208	OP482278
R. camporesii	HKAS 104277^{T}	MN429072	MN429069	MN442087	NA
R. chromolaenae	MFLUCC 17-1516^{T}	MN632456	MN632461	MN635663	MN632467
R. coffeae	KUMCC 21-0492	OP526406	OP605963	OP572201	OP526412
R. coffeae	KUMCC 21-0489^{T}	OP526407	OP605964	OP572202	OP526413
R. cozumelense	A. Cobos-Villagrán951	MW939459	MZ056797	MZ457338	NA
R. cozumelense	T. Raymundo 7321	MW939460	MZ056798	MZ457339	NA
R. erioi	MFLU 16-0584^{T}	MN429071	MN429068	MN442086	NA
R. esperanzae	T. Raymundo 6579	MZ477203	MZ056795	MZ457336	NA
R. esperanzae	R. Valenzuela 17206	MZ477204	MZ056796	MZ457337	NA
R. hongheense	KUMCC 21-0487	OP482287	OP494092	OP572209	OP482279
R. hongheense	KUMCC 20-0222	MW264193	MW264214	MW256815	MW264223
R. hongheense	HKAS112348	MW541820	MW541824	MW556132	MW541831

Fungal Species	Strain numbers	LSU	ITS	*tef*1-α	SSU
R. hongheense	HKAS112349	MW541821	MW541825	MW556133	MW541832
R. hysterinum	EB 0351	GU397350	NA	GU397340	NA
R. hysterinum	CBS 316.71	MH871912	MH860141	NA	NA
R. ligustrum	SICAUCC 20-0004^{T}	MT062446	MT062850	MT075600	MT062451
R. ligustrum	SICAUCC 19-0007	MN956789	MN956777	MT027603	MN956798
R. magnoliae	KUMCC 21-0478	OP482288	OP494093	OP572210	OP482280
R. magnoliae	MFLUCC 18-0719^{T}	MN989384	MN989383	MN997309	MN989382
R. mangrovei	MFLU 18-1894^{T}	MK357777	MK425188	MK450030	NA
R. mengziense	KUMCC 21-0490^{T}	OP526396	OP526402	OP572203	OP526414
R. mengziense	KUMCC 21-0491	OP526397	OP526403	OP572204	OP526415
R. mesophilum	A. Trejo 74	MW939461	MZ056799	MZ457340	NA
R. mesophilum	A. Cobos-Villagrán 1800	MW939462	MZ056800	MZ457341	NA
R. mexicanum	RV17107.1^{T}	MT626028	MT626026	NA	NA
R. mexicanum	RV17107.2	MT626029	MT626027	NA	NA
R. neorufulum	KUMCC 21-0480	OP482290	OP494095	OP572212	OP482282
R. neorufulum	MFLUCC 21-0035	MZ346015	MZ346025	MZ356249	MZ346020
R. neorufulum	MFLUCC 13-0216^{T}	KU377566	KU377561	KU510400	KU377571
R. neorufulum	GKM 361A	GQ221893	NA	NA	GU296192
R. neorufulum	HUEFS 192194	KF914915	NA	NA	NA
R. neorufulum	MFLUCC 12-0528	KJ418117	KJ418118	NA	KJ418119
R. neorufulum	CBS 306.38	FJ469672	NA	GU349031	GU296191
R. neorufulum	MFLUCC 12-0011	KJ418109	KJ206287	NA	KJ418110
R. neorufulum	MFLUCC 12-0567	KJ526126	KJ546124	NA	KJ546129
R. neorufulum	MFLUCC 12-0569	KJ526128	KJ546126	NA	KJ546131
R. neorufulum	EB 0381	GU397351	NA	NA	GU397366
R. opuntiae	GKM 1190	GQ221892	NA	GU397341	NA
R. rufulum	MFLUCC 14-0577^{T}	KU377565	KU377560	KU510399	KU377570
R. rufulum	EB 0384	GU397354	NA	NA	GU397368
R. rufulum	EB 0382	GU397352	NA	NA	NA
R. rufulum	EB 0383	GU397353	NA	NA	GU397367
R. rufulum	MFLUCC 12-0013	KJ418111	KJ418112	NA	KJ418113
R. sichuanense	SICAUCC 19-0005^{T}	MN956787	MN956775	MT027601	MN956796
R. sichuanense	SICAUCC 19-0006	MN956788	MN956776	MT027602	MN956797
R. sichuanense	SICAUCC 20-0005	MT062447	MT062851	MT075601	MT062452
R. subrufulum	SICAUCC 19-0011^{T}	MN956793	MN956781	MT027607	MN956802
R. subrufulum	SICAUCC 19-0010	MN956792	MN956780	MT027606	MN956801
R. subrufulum	SICAUCC 20-0003	MT062445	MT062849	MT075599	MT062450
R. tectonae	KUMCC 21-0479	OP482291	OP494096	OP572213	OP482283
R. tectonae	MFLUCC 21-0037	MZ346013	MZ346023	MZ356247	MZ346018
R. tectonae	MFLUCC 21-0034	MZ346014	MZ346024	MZ356248	MZ346019
R. tectonae	MFLUCC 13-0710^{T}	KU764698	KU144936	KU872760	KU712457
R. thailandicum	KUMCC 21-0493	OP482292	OP494097	OP572214	OP482284
R. thailandicum	MFLUCC 14-0503^{T}	KU377564	KU377559	KU497490	KU377569
R. thailandicum	MFLUCC 12-0530	KJ526125	KJ546123	NA	KJ546128
R. thailandicum	MFLU17-0788	MT093472	MT093733	NA	MT093495
R. thailandicum	MFLUCC 13-0051	MN509434	MN509433	MN509435	NA
R. xiaokongense	KUMCC 20-0158	MZ346011	MZ346021	MZ356245	MZ346016
R. xiaokongense	KUMCC 20-0160^{T}	MZ346012	NR_185637	MZ356246	NG_242421
R. xizangense	**GZCC 25-0851^{T}**	**PX413306**	**PX561053**	**PX425314**	**PX413301**
R. xizangense	**GZCC 25-0852**	**PX413307**	**NA**	**PX436846**	**PX413302**
R. yunnanense	KUMCC 21-0485^{T}	OP526404	OP526410	OP572205	OP526400
R. yunnanense	KUMCC 21-0486	OP526405	OP526411	OP572206	OP526401

Taxonomy and results

Phylogenetic analyses of *Hermatomyces*

The concatenated dataset includes 53 strains, including the new collections. The best-scoring RAxML tree is shown in Fig. 1, with a final likelihood value of −15404.961825. The alignment contains a total of 3,809 characters (with gaps included), distributed as follows: ITS (1–503), LSU (504–1,320), *rpb*2 (1,321–2,325), *tef*1-α (2,326–3,249), and *tub*2 (3,250–3,809). The tree was

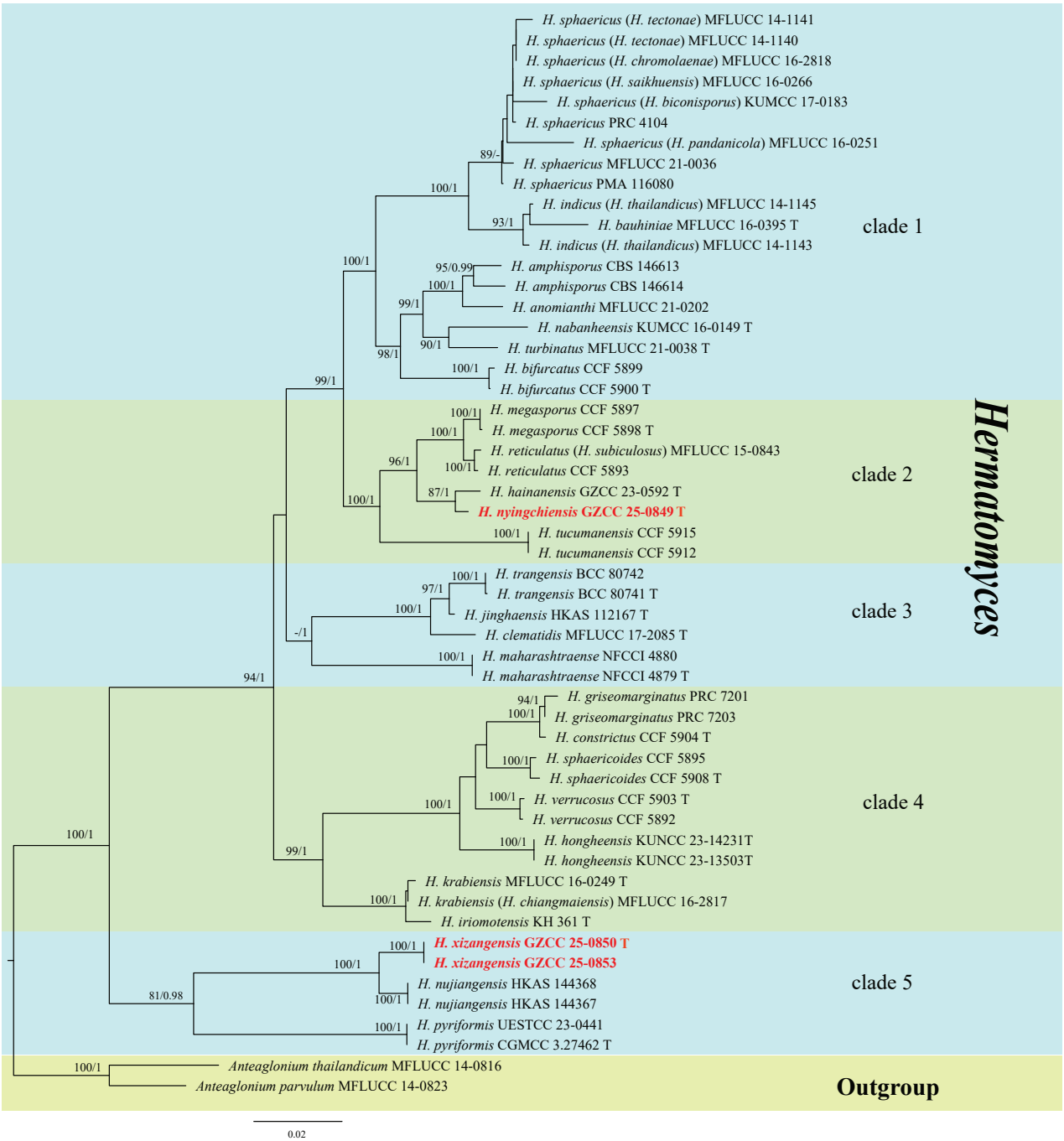

Figure 1. The ML tree based on a combined dataset of LSU, ITS, *tef*1-α, *rpb*2 and *tub*2 sequences. Bootstrap support values for ML greater than 75% and PP greater than 0.95 are marked near each node as ML/PP. Newly generated isolates are highlighted in bold red.

rooted with *Anteaglonium parvulum* (MFLUCC 14-0823) and *A. thailandicum* (MFLUCC 14-0816). The alignment matrix exhibited 1,110 distinct patterns, with undetermined characters or gaps constituting 24.90% of the total dataset. Phylogenetic trees derived from ML and BI analyses exhibited fundamentally comparable topologies.

In the phylogenetic tree (Fig. 1), our strain of *Hermatomyces nyingchiensis* (GZCC 25-0849) formed a distinct clade that was sister to *H. hannanensis* (GZCC 23-0592) with 87% ML and 1 PP support. Our two strains of *Hermatomyces xizangensis* (GZCC 25-0850 and GZCC 25-0853) grouped together, forming a distinct clade sister to *H. nujiangensis* (HKAS 144367 and HKAS 144368) with 100% ML and 1 PP support.

Hermatomyces nyingchiensis **G.L. Zhao, N.G. Liu & Y.Z. Lu, sp. nov.**

Fungal Names: FN 573085

Fig. 2

Etymology. Referring to the location Nyingchi City, where the holotype was collected.

Holotype. HKAS 149901.

Description. ***Saprobic*** on dead vine of *Pueraria* sp. in a terrestrial habitat. ***Sexual morph*** Undetermined. ***Asexual morph*** Hyphomycetous. *Colonies* on natural substrates superficial, effuse, scattered, comprising a greenish brown sterile mycelial outer region, and a dark brown to blackish brown center. ***Mycelium*** partly immersed and partly superficial, consisting of pale to brown, branched hyphae. ***Conidiophores*** micronematous, mononematous, geniculate, hyaline to pale brown, septate, thick-walled. ***Conidiogenous cells*** monoblastic, integrated, terminal, hyaline to pale brown. ***Conidia*** dimorphic, (1) cylindrical conidia 36–42 × 14–17 µm ($\overline{x}$ = 38 × 15 µm, n = 15), hyaline to subhyaline, frequently exhibiting a distinct dark brown pigment, which either extends from the top downward or at the conidial rim, straight or broadly curved, phragmoseptate or muriform, with oblique septa occasionally present, constricted at septa, composed of two columns arising from one or two basal cells. (2) lenticular conidia 30–40 × 23–29 µm ($\overline{x}$ = 35 × 27 µm, n = 30), 16–21 µm thick ($\overline{x}$ = 18.5 µm, n = 10), in front view, subglobose to ellipsoidal, or slightly irregular, peripheral cells pale brown to brown, forming a distinct ring, constricted at the septa, central cells dark brown, in side view, rugby-shaped, oval, two distinct adpressed halves can be recognized, each half arranged by 6–10 cells, end cells subhyaline to pale brown, middle cells dark brown.

Culture characteristics. Conidial germination was observed within 24 hours incubated on PDA medium at 28 °C. Colony reached a diameter of 1.9 cm after 19 days at room temperature, circular, dense, convex at the center, margin entire, pale brown on the front, dark brown in reverse.

Material examined. China, Xizang Autonomous Region, Nyingchi City, Bomi County, (30°3'16"N, 95°12'20"E, 2320 m), on dead vine of *Pueraria* sp., 26 July 2024, G.L. Zhao, DDQGF14A (HKAS 149901, holotype), DDQGF14B **(**HKAS 149903, isotype**)**, ex-type culture GZCC 25-0849.

Notes. *Hermatomyces nyingchiensis* resembles those *Hermatomyces* species that possess dimorphic conidia (Tibpromma et al. 2016; Hashimoto et al.

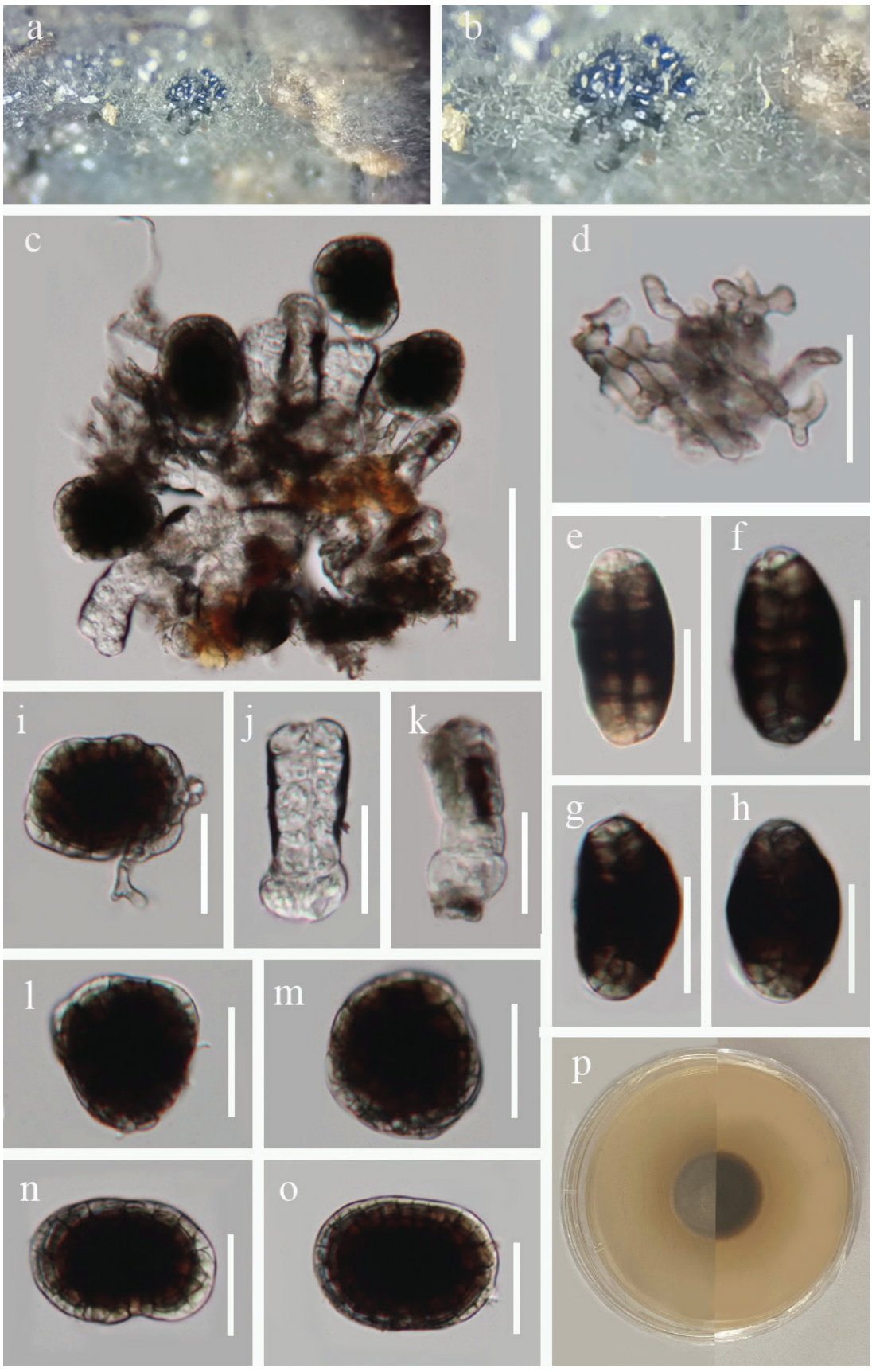

Figure 2. *Hermatomyces nyingchiensis* (HKAS 149901, holotype). **a, b.** Colonies on natural substrates; **c.** Conidial mass; **d.** Subicular hyphae; **e–h.** Lenticular conidia (side view); **i.** Conidiophore with conidium; **j, k.** Cylindrical conidia; **l–o.** Lenticular conidia (front view); **p.** Colony on PDA (left from above, right from below). Scale bars: 50 μm (**c**); 20 μm (**d–o**).

2017; Koukol et al. 2018; Ren et al. 2021; Zhang et al. 2023). In the phylogenetic tree (Fig. 1), our isolate (GZCC 25-0849) formed a distinct clade and was sister to *H. hainanensis* (GZCC 23-0592) with 87% ML-BS and 1 PP support (Fig. 1). However, the two conidial types of *H. nyingchiensis* are smaller than those of *H. hainanensis*: (1) cylindrical conidia, 36–42 × 14–17 µm vs. 51–67 × 16–24 µm; and (2) lenticular conidia, 30–40 × 23–29 µm vs. 44–52 × 29–39 µm (Zhang et al. 2023). Therefore, based on phylogenetic analyses and morphological characteristics, *H. nyingchiensis* is identified as a new species.

Hermatomyces xizangensis **G.L. Zhao, N.G. Liu & Y.Z. Lu, sp. nov.**
Fungal Names: FN 573046
Fig. 3

Etymology. Referring to the location Xizang Autonomous Region, where the fungus was collected.

Holotype. HKAS 149902.

Description. ***Saprobic*** on dead vine of *Pueraria* sp. in a terrestrial habitat. ***Sexual morph*** Undetermined. ***Asexual morph*** Hyphomycetous. ***Colonies*** on natural substrate sporodochial, superficial, scattered, effuse, consisting of a velvety, sparse, brown sterile mycelial outer zone enclosing a brown to black, glistening, abundantly sporulating center, conidia not easily dislodged when disturbed. ***Mycelium*** mostly immersed and consisting of branched, smooth, septate, brown hyphae. ***Conidiophores*** micronematous, mononematous, curved, unbranched, light brown to brown thick-walled. ***Conidiogenous cells*** monoblastic, integrated, terminal, subcylindrical, hyaline to brown. ***Conidia*** 26–48 × 17–39 µm ($\bar{x}$ = 36 × 27 µm, n = 30), 13–20 µm thick ($\bar{x}$ = 15.5 µm, n = 15), monomorphic, lenticular, dry muriform, smooth, in front view, ellipsoidal, peripheral cells pale brown to brown, forming a distinct ring, constricted at the septa, central cells dark brown to blackish brown, in side view, rugby-shaped, oval, two distinct adpressed halves can be recognized, each half arranged by 8–10 cells, end cells subhyaline to pale brown, middle cells brown to dark brown.

Culture characteristics. Conidia germinated within 24 hours on PDA medium at 28 °C. The colony reached 1.8 cm diam after 13 days at room temperature, circular, dense, bulge at middle with entire margin, reverse brown, with a lighter coloration at the margins and a darker pigmentation toward the center.

Material examined. China, Xizang Autonomous Region, Nyingchi City, Bomi County, (30°3'16"N, 95°12'20"E, 2320 m), on dead vines of *Pueraria* sp., 26 July 2024, G.L. Zhao, DDQGF12A (HKAS 149902, holotype), ex-type culture GZCC 25-0850; *ibid*., DDQGF12B (HKAS 149904, isotype), ex-isotype culture GZCC 25-0853.

Notes. Based on multi-gene phylogenetic analysis, our collections of *Hermatomyces xizangensis* (GZCC 25-0850 and GZCC 25-0853) formed an independent clade, sister to *H. nujiangensis* (HKAS 144367 and HKAS 144368) with 100% ML and 1 PP support (Fig. 1). Morphologically, conidia of *H. xizangensis* consist of 8–10 cells per half in side view, whereas those of *H. nujiangensis* have 15–22 cells (Yang et al. 2025). Furthermore, three *Hermatomyces* species, viz., *H. dimorphus*, *H. uniseriatus*, and *H. truncatus*, for which molecular data are lacking, are characterized by dimorphic conidia, including both lenticular and cylindrical types (Rao and de Hoog 1986; Leão-Ferreira et al. 2013;

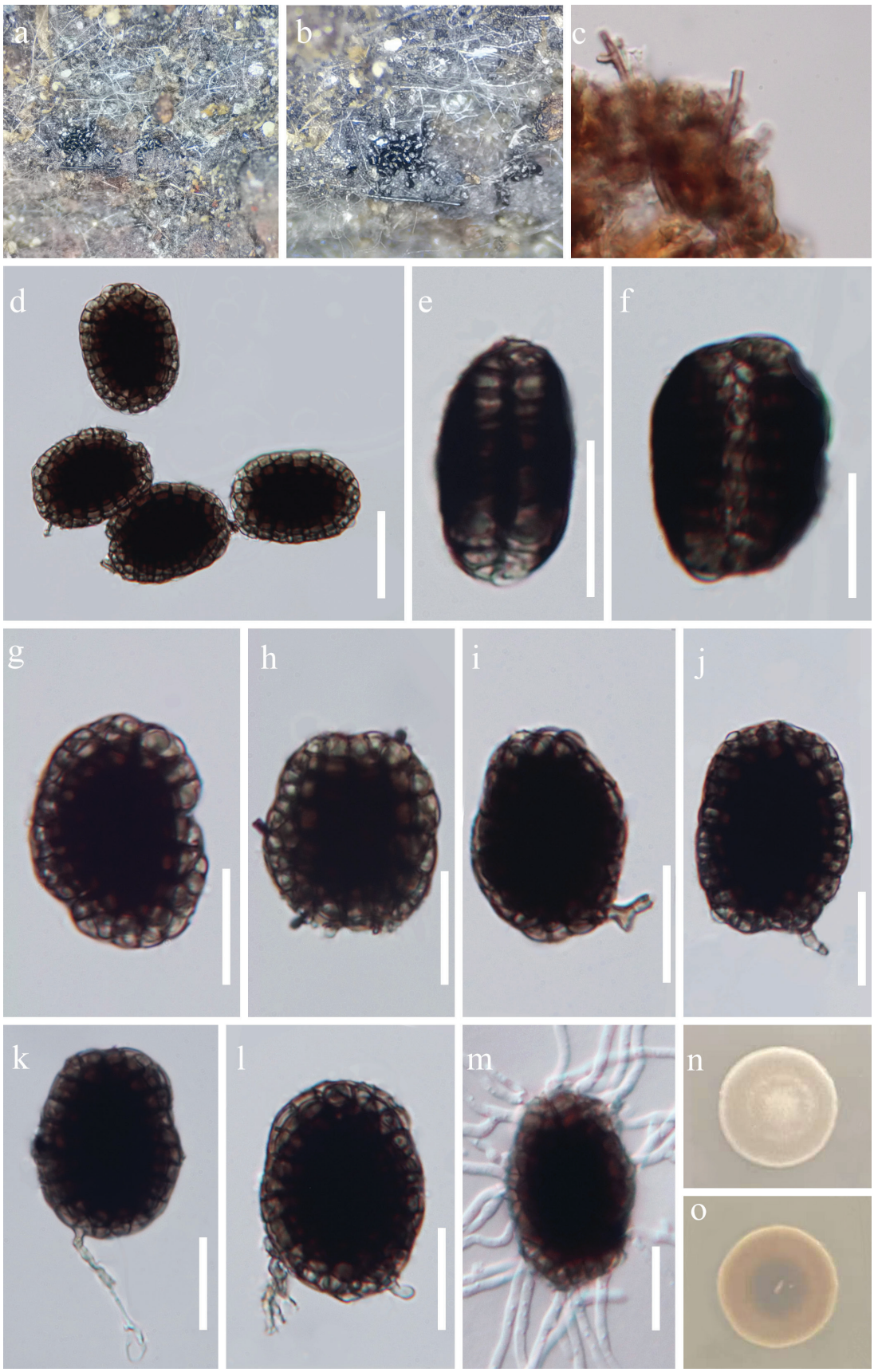

Figure 3. *Hermatomyces xizangensis* (HKAS 149902, holotype). **a, b.** Colonies on natural substrates; **c.** Subicular hyphae; **d–l.** Conidiophores and conidia; **m.** Germinated conidium; **n, o.** Colony on PDA (**n.** From above; **o.** From below). Scale bars: 50 µm (**d**); 20 µm (**e–m**).

Koukol and Delgado 2019). In contrast, *H. xizangensis* produces only lenticular conidia. Therefore, based on molecular evidence and morphological comparisons, *H. xizangensis* is identified as a new species.

Phylogenetic analyses of *Rhytidhysteron*

The final ML tree of *Rhytidhysteron* exhibited a topological pattern congruent with that reported by Du et al. (2023). The tree was constructed using a concatenated dataset composed of four gene regions: ITS, LSU, SSU, and *tef*1-α, totaling 3,280 aligned characters (including gaps). The partitioning scheme was as follows: ITS (1–579), LSU (580–1,433), SSU (1,434–2,427), and *tef*1-α (2,428–3,280). *Gloniopsis calami* (MFLUCC 15-0739) and *G. praelonga* (CBS 112415) were selected as outgroup taxa. The ML analysis of the concatenated matrix yielded the best-scoring tree (Fig. 4) with a final optimization likelihood score of −11534.338749. The matrix had 831 distinct alignment patterns, and undetermined characters or gaps accounted for 20.42% of the total.

Within *Rhytidhysteron*, our new taxon, *R. xizangense* constitutes a distinct clade and is sister to *R. hysterinum* (EB 0351 and CBS 316.71).

Rhytidhysteron xizangense **G.L. Zhao, N.G. Liu & Y.Z. Lu, sp. nov.**
Fungal Names: FN 573045
Figs 5, 6

Etymology. Referring to the Xizang Autonomous Region, where the holotype was collected.

Holotype. HKAS 149907.

Description. ***Saprobic*** on dead vine of *Pueraria* sp. in a terrestrial habitat. **Sexual morph** ***Ascomata*** 1432–1818 µm long × 780–1265 µm wide × 648–1100 µm high ($\bar{x}$ = 1622 × 959 × 822 µm, n = 5), scattered to gregarious, semi-immersed to superficial, hysterothecial, bilabiate, closed, black, perpendicular striae. ***Exciple*** 150–220 µm ($\bar{x}$ = 170 µm, n = 5) wide, consisting of dark brown, thick-walled cells arranged in a *textura angularis* structure, outer layer brown to dark brown, inner layer hyaline. ***Hamathecium*** 2–3 µm ($\bar{x}$ = 2.5, n = 10) wide at the base, 3.5–6.5 µm ($\bar{x}$ = 4.5, n = 10) wide at swollen tips, dense, brown at the swollen apex, hyaline at the base, septate, branched, pseudoparaphyses, forming a brown epithecium above the asci, swollen with dense septa at the apex. ***Asci*** 199–275 × 13–18 µm ($\bar{x}$ = 224 × 16 µm, n = 20), 8-spored, bitunicate, clavate to cylindrical, short pedicel, rounded at the apex, with an ocular chamber. ***Ascospores*** 23–30 × 9–14 µm ($\bar{x}$ = 26.5 × 11 µm, n = 30), uni-seriate, slightly overlapping, 1-septate, hyaline when immature, brown to dark brown when mature, fusiform to ellipsoidal, slightly pointed at both ends, thick-walled. ***Asexual morph*** Sporulation in PDA media, coelomycetous. ***Conidiomata*** 260–519 µm high × 391–467 µm wide ($\bar{x}$ = 411 × 424 µm, n = 10), superficial, subglobose, solitary or aggregated, dark brown to black, thick-walled. ***Conidiomata wall*** 63–288 µm ($\bar{x}$ = 124 µm, n = 15) wide, consisting of brown, thick-walled cells arranged in a *textura angularis* structure. ***Conidia*** 2.5–4.5 µm diam. ($\bar{x}$ = 3.0 µm, n = 40), globose, hyaline, smooth-walled.

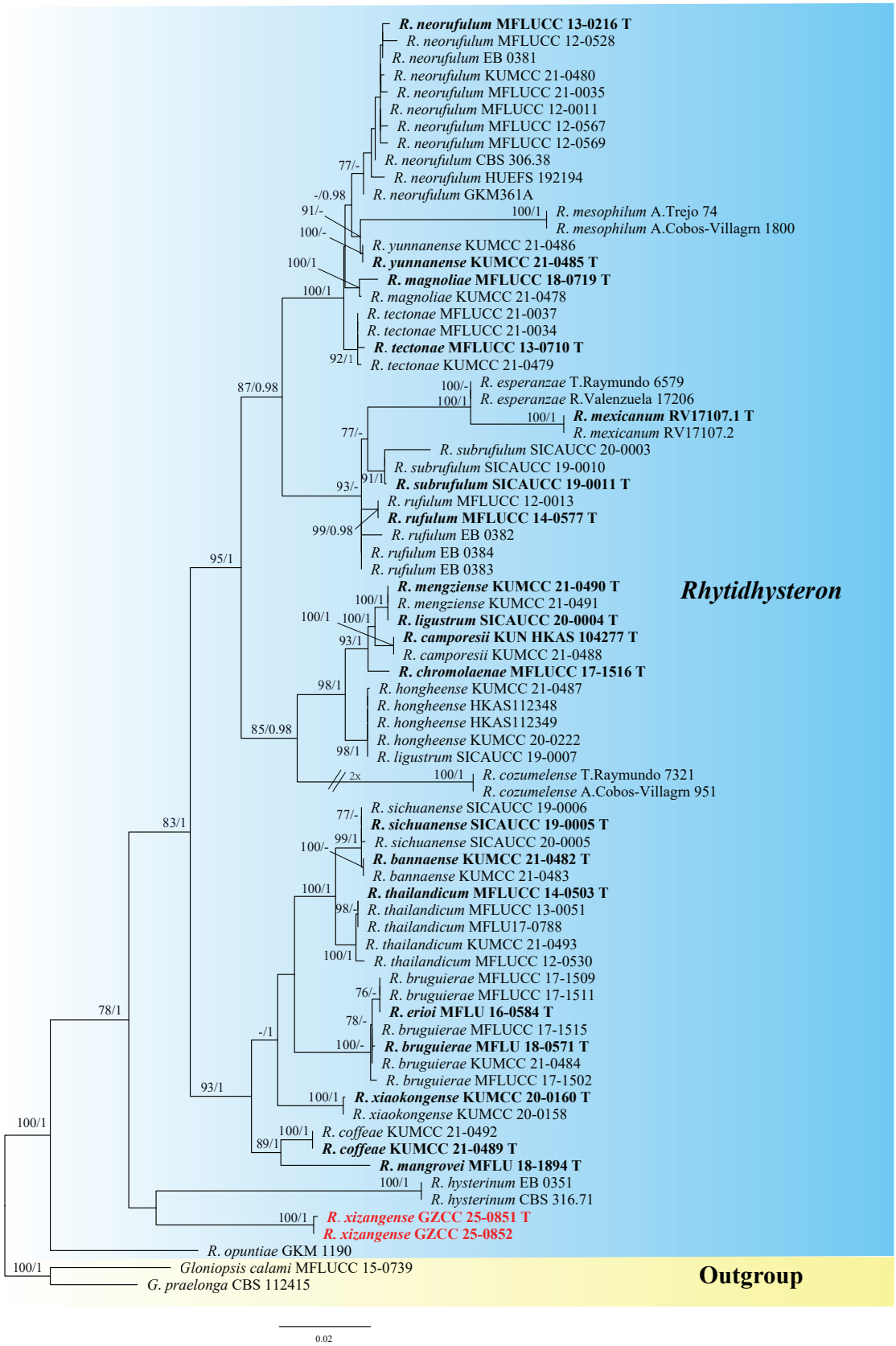

Figure 4. Phylogenetic tree from ML analysis based on the combined ITS, LSU, SSU, and *tef*1-α sequence datasets. Bootstrap support values for ML greater than 75% and PP greater than 0.95 are marked near each node as ML/PP. Newly generated isolates are highlighted in bold red.

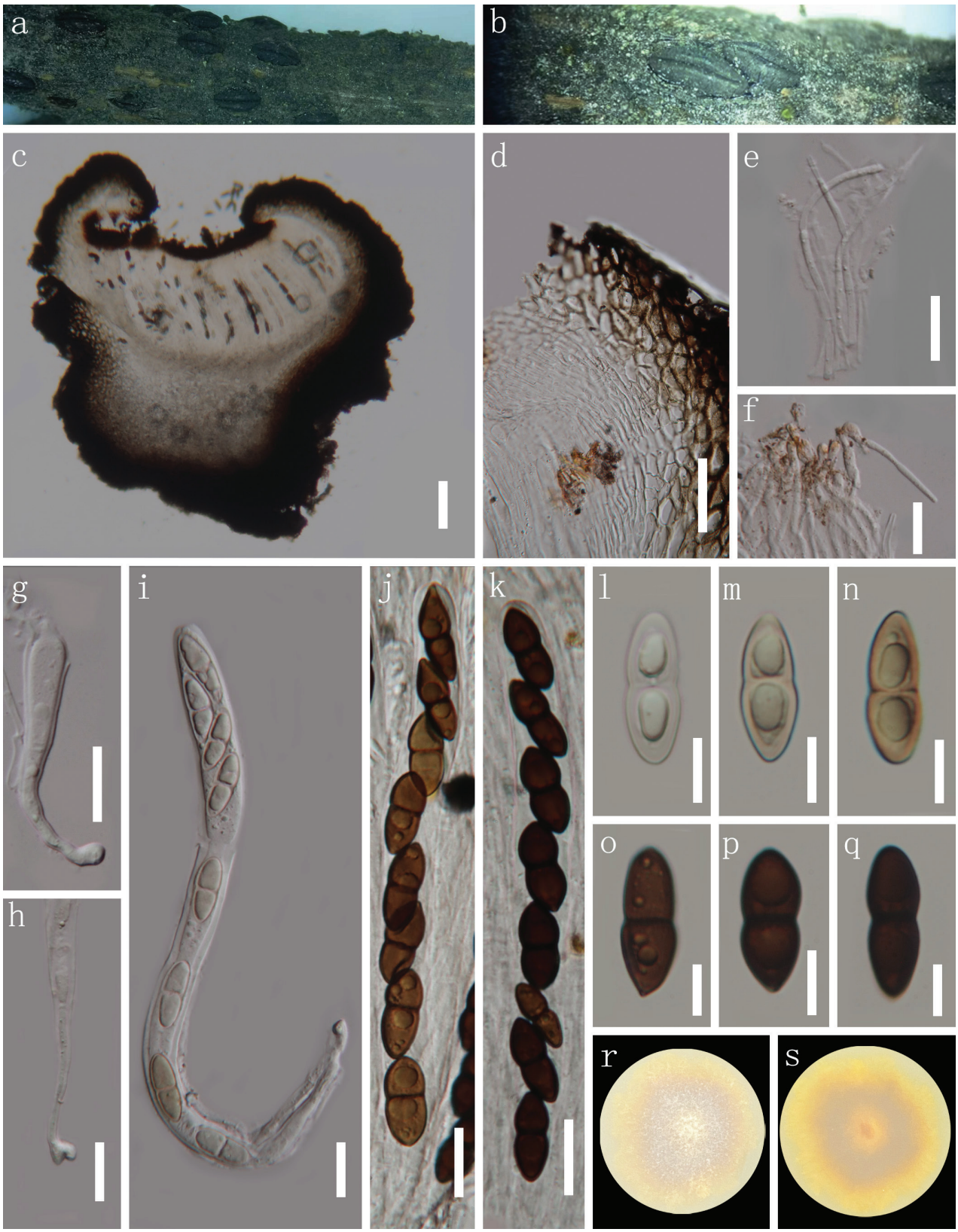

Figure 5. *Rhytidhysteron xizangense* (HKAS 149907, holotype). **a, b.** Appearance of hysterothecia on the host; **c.** Vertical section through hysterothecium; **d.** Exciple; **e.** Pseudoparaphyses; **f.** Epithecium mounted in water; **g, h.** Pedicel of asci; **i–k.** Asci; **l–q.** Ascospores; **r, s.** Colony on PDA medium. Scale bars: 100 µm (**c**); 50 µm (**d**); 20 µm (**e–k**); 10 µm (**l–q**).

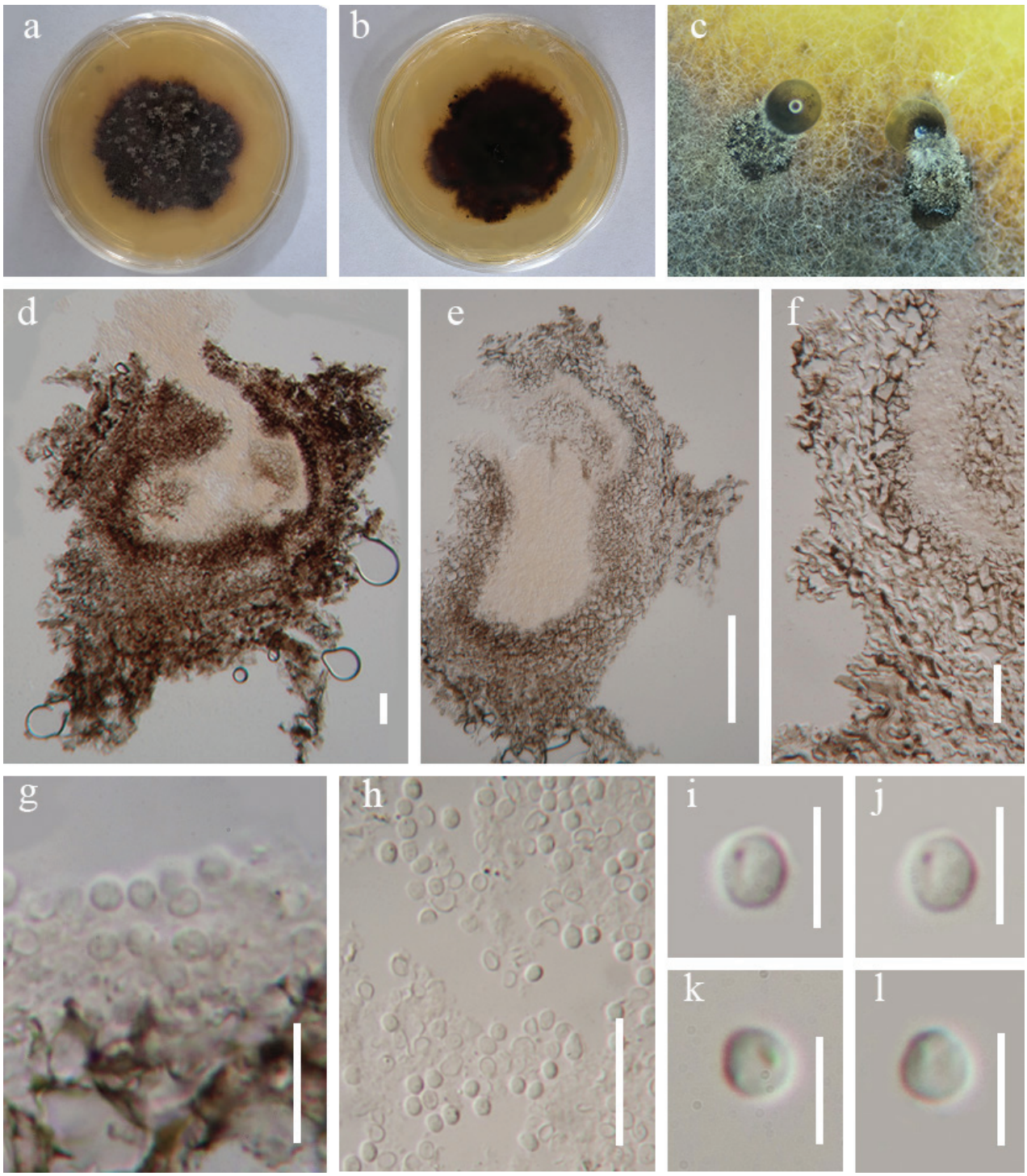

Figure 6. *Rhytidhysteron xizangense* (HKAS 149907, holotype) on PDA. **a, b.** Obverse and reverse colony on PDA; **c.** Conidiomata on PDA; **d, e.** Vertical section through conidiomata; **f, h.** Conidiomatal wall; **g, h.** Conidiogenous cells and conidia; **i–l.** Conidia. Scale bars: 100 µm (**d, e**); 20 µm (**f, h**); 10 µm (**g**); 5 µm (**i–l**).

Culture characteristics. Conidia germinated within 24 hours on PDA medium at 28 °C. After one month of incubation at room temperature, colonies reached a diameter of 3.35 cm. Colonies velvety, subrounded, with wavy margins, yellow in the center, brown in the middle, with light yellow at the edge.

Material examined. CHINA, Xizang Autonomous Region, Nyingchi City, Bomi County (29°53'11"N, 95°42'9"E, 2720 m), on dead vine of *Pueraria* sp., 26 July 2024, G.L. Zhao, CGGF7A (holotype, HKAS 149907), ex-type living culture GZCC 25-0851; *ibid*., CGGF7B (isotype, HKAS 149908), ex-isotype living culture GZCC 25-0852.

Notes. *Rhytidhysteron xizangense* is similar to *R. neohysterinum* in the shapes of ascomata, asci, and ascospores (Cobos-Villagrán et al. 2020). However, in the phylogenetic tree (Fig. 4), *R. xizangense* (GZCC 25-0851 and GZCC 25-0852) formed an independent clade and is sister to *R. hysterinum* (EB 0351 and CBS 316.71). BLAST analyses of the ITS and LSU sequences revealed that our strain (GZCC 25-0851) shares 92% (36/439, including 8 gaps) and 97% (21/786, including 0 gap) similarity with *R. hysterinum* (CBS 316.71), respectively. Morphologically, *Rhytidhysteron xizangense* differs from *R. hysterinum* by its larger ascomata (780–1265 µm vs. 500 µm) (Thambugala et al. 2016; Ren et al. 2022; Du et al. 2023). Therefore, based on molecular data and morphological comparisons, we introduce *Rhytidhysteron xizangense* as a new species.

Discussion

In this study, three novel species, namely *Hermatomyces nyingchiensis*, *H. xizangensis*, and *Rhytidhysteron xizangense*, are introduced. These collections were isolated from decaying vines of *Pueraria* sp. in the Xizang Autonomous Region. The findings of this study further clarify the species diversity within *Hermatomyces* and *Rhytidhysteron* while also supplementing the distribution information of fungi associated with *Pueraria* hosts.

Among the 26 recognized species of *Hermatomyces* (Table 1), 15 species exhibit conidial dimorphism, such as *H. amphisporus*, *H. bifurcatus*, *H. hainanensis*, *H. nabanheensis*, and *H. turbinatus* (Hyde et al. 2017; Koukol et al. 2018; Delgado et al. 2020; Ren et al. 2021; Zhang et al. 2023). Nine species produce exclusively monomorphic conidia, viz., *H. griseomarginatus*, *H. hongheensis*, *H. maharashtraense*, *H. pyriformis*, *H. reticulatus*, *H. sphaericoides*, *H. trangensis*, *H. verrucosus*, and *H. xizangensis* (Koukol et al. 2018, 2025; Nuankaew et al. 2019; Wijayawardene et al. 2021; Du et al. 2024; Shen et al. 2024). One species, *H. sphaericus*, is known to exhibit either monomorphic or dimorphic conidia (Doilom et al. 2016; Tibpromma et al. 2016, 2017, 2018; Koukol et al. 2018; Ren et al. 2021), whereas *H. anomianthi* is known solely from its sexual morph (de Silva et al. 2022). Phylogenetic analysis indicates that conidial morphology (monomorphic vs. dimorphic) does not exhibit a clear phylogenetic clustering pattern. For instance, *H. megasporus* (dimorphic conidia) and *H. reticulatus* (monomorphic conidia) cluster in clade 2 (Fig. 1) (Hyde et al. 2016; Koukol et al. 2018), while *H. jinghaensis* (dimorphic conidia) and *H. trangensis* (monomorphic conidia) also group together in clade 3 (Fig. 1) (Nuankaew et al. 2019; Ren et al. 2021). Furthermore, conidial type shows no significant correlation with biogeographical distribution. Although both *H. hongheensis* and *H. nabanheensis* were collected from Yunnan, China, the former produces monomorphic conidia, whereas the latter develops dimorphic conidia (Hyde et al. 2017; Shen et al. 2024). To elucidate the underlying mechanisms governing the formation of dimorphic conidia and monomorphic conidia in *Hermatomyces*, broader sampling is essential across diverse geographical regions, ecologi-

cal niches, and developmental stages. Future research integrating comparative genomics, transcriptomics, and ecological niche modeling will be crucial for elucidating the evolutionary and ecological drivers of conidial dimorphism within the genus.

Acknowledgments

We would like to thank Yuan-Pin Xiao, Dan-Feng Bao, Xue-Yan Chen, and Li-Juan Luo for their help with this study.

Additional information

Conflict of interest

The authors have declared that no competing interests exist.

Ethical statement

No ethical statement was reported.

Use of AI

No use of AI was reported.

Funding

This study was supported by the Guizhou Institute of Technology 2024 Annual Academic Seedling Cultivation and Innovation Exploration Project (No. 2024XSXM001, 2024XSXM010), the Science and Technology Foundation of Guizhou Province (Qian Ke He Pingtai ZSYS [2025] 029), the Guizhou Provincial Basic Research Program (Natural Science) (Qiankehe Jichu ZK [2023] yiban 132), and the Guizhou Science and Technology Plan Project (Qiankehe Support [2023] Generally 295).

Author contributions

Morphological data, photo plates, and phylogenetic analyses were completed by Gui-Li Zhao. Writing – original draft: Gui-Li Zhao. Writing – review and editing: all co-authors.

Author ORCIDs

Gui-Li Zhao https://orcid.org/0000-0001-8370-4844
Yong-Zhong Lu https://orcid.org/0000-0002-1033-5782
Xing-Juan Xiao https://orcid.org/0009-0003-8769-4534
Ying Liu https://orcid.org/0009-0003-4850-4929
Qiang Chen https://orcid.org/0009-0004-2035-6562
Ning-Guo Liu https://orcid.org/0000-0002-9169-2350

Data availability

All of the data that support the findings of this study are available in the main text.

References

Bezerra JL, Kimbrough JW (1982) Culture and cytological development of *Rhytidhysterium rufulum* on citrus. Canadian Journal of Botany 60(5): 568–579. https://doi.org/10.1139/b82-078

Boehm EW, Schoch CL, Spatafora JW (2009) On the evolution of the Hysteriaceae and Mytilinidiaceae (Pleosporomycetidae, Dothideomycetes, Ascomycota) using four nuclear genes. Mycological Research 113: 461–479. https://doi.org/10.1016/j.mycres.2008.12.001

Capella-Gutiérrez S, Silla-Martinez JM, Gabaldon T (2009) TrimAl: A tool for automated alignment trimming in large-scale phylogenetic analyses. Bioinformatics 25(15): 1972–1973. https://doi.org/10.1093/bioinformatics/btp348

Chen X, Yu J, Shi J (2018) Management of diabetes mellitus with puerarin, a natural isoflavone from *Pueraria lobata*. The American Journal of Chinese Medicine 46(8): 1771–1789. https://doi.org/10.1142/S0192415X18500891

Chen F, Chen ZQ, Wang H, Zhu JJ (2021) Puerarin pretreatment inhibits myocardial apoptosis and improves cardiac function in rats after acute myocardial infarction through the PI3K/Akt signaling pathway. Advances in Clinical and Experimental Medicine 30(3): 255–261. https://doi.org/10.17219/acem/131754

Clewley JP (1995) Macintosh sequence analysis software – DNAStar's LaserGene. Molecular Biotechnology 3: 221–224. https://doi.org/10.1007/BF02789332

Cobos-Villagrán A, Hernández-Rodríguez C, Valenzuela R, Villa-Tanaca L, Calvillo-Medina RP, Mateo-Cid LE, MartínezPineda M, Raymundo T (2020) El género *Rhytidhysteron* (Dothideomycetes, Ascomycota) en México. Acta Botánica Mexicana 127: e1675. https://doi.org/10.21829/abm127.2020.1675

de Silva NI, Tennakoon DS, Thambugala KM, Karunarathna SC, Lumyong S, Hyde KD (2020) Morphology and multigene phylogeny reveal a new species and a new record of *Rhytidhysteron* (Dothideomycetes, Ascomycota) from China. Asian Journal of Mycology 3(1): 295–306. https://doi.org/10.5943/ajom/3/1/4

de Silva NI, Hyde KD, Lumyong S, Phillips AJL, Bhat DJ, Maharachchikumbura SSN, Thambugala KM, Tennakoon DS, Suwannarach N, Karunarathna SC (2022) Morphology, phylogeny, host association and geography of fungi associated with plants of Annonaceae, Apocynaceae and Magnoliaceae. Mycosphere: Journal of Fungal Biology 13(1): 955–1076. https://doi.org/10.5943/mycosphere/13/1/12

Delgado G, Koukol O, Heredia G, Piepenbring M (2020) Texas microfungi: *Hermatomyces amphisporus* (Pleosporales, Dothideomycetes) revisited. Czech Mycology 72(1): 95–107. https://doi.org/10.33585/cmy.72107

Dissanayake AJ, Bhunjun CS, Maharachchikumbura SSN, Liu JK (2020) Applied aspects of methods to infer phylogenetic relationships amongst fungi. Mycosphere: Journal of Fungal Biology 11: 2652–2676. https://doi.org/10.5943/mycosphere/11/1/18

Doilom M, Dissanayake AJ, Wanasinghe DN, Boonmee S, Liu JK, Bhat DJ, Taylor JE, Bahkali AH, McKenzie EHC, Hyde KD (2016) Microfungi on Tectona grandis (teak) in Northern Thailand. Fungal Diversity 82: 107–182. https://doi.org/10.1007/s13225-016-0368-7

Du TY, Dai DQ, Mapook A, Lu L, Stephenson SL, Suwannarach N, Tibpromma S (2023) Additions to *Rhytidhysteron* (Hysteriales, Dothideomycetes) in China. Journal of Fungi 9(2): e148. https://doi.org/10.3390/jof9020148

Du HZ, Liu NG, Cheewangkoon R, Liu JK (2024) *Hermatomyces pyriformis* sp. nov., a novel dematiaceous hyphomycete (Hermatomycetaceae, Pleosporales) associated with medicinal plants in Yunnan Province, China. Phytotaxa 650(1): 103–115. https://doi.org/10.11646/phytotaxa.650.1.9

Guo Y, Bei Q, Dzomeku BM, Martin K, Rasche F (2022) Genetic diversity and community composition of arbuscular mycorrhizal fungi associated with root and rhizo-

sphere soil of the pioneer plant *Pueraria phaseoloides*. iMeta 1(4): e51. https://doi.org/10.1002/imt2.51

Hashimoto A, Matsumura M, Hirayama K, Tanaka K (2017) Revision of Lophiotremataceae (Pleosporales, Dothideomycetes): Aquasubmersaceae, Cryptocoryneaceae, and Hermatomycetaceae fam. nov. Persoonia 39: 51–73. https://doi.org/10.3767/persoonia.2017.39.03

Hyde KD, Hongsanan S, Jeewon R, Bhat DJ, McKenzie EHC, Jones EBG, Phookamsak R, Ariyawansa HA, Boonmee S, Zhao Q, Abdel-Aziz FA, Abdel-Wahab MA, Bannmai S, Chomnunti P, Cui BK, Daranagama DA, Das K, Dayarathne MC, de Silva NI, Dissanayake AJ, Doilom M, Ekanayaka AH, Gibertoni TB, Góes-Neto A, Huang SK, Jayasiri SC, Jayawardena RS, Konta S, Lee HB, Li WJ, Lin CG, Liu JK, Lu YZ, Luo ZL, Manawasinghe IS, Manimohan P, Mapook A, Niskanen T, Norphanphoun C, Papizadeh M, Perera RH, Phukhamsakda C, Richter C, de A. Santiago ALCM, Drechsler-Santos ER, Senanayake IC, Tanaka K, Tennakoon TMDS, Thambugala KM, Tian Q, Tibpromma S, Thongbai B, Vizzini A, Wanasinghe DN, Wijayawardene NN, Wu HX, Yang J, Zeng XY, Zhang H, Zhang JF, Bulgakov TS, Camporesi E, Bahkali AH, Amoozegar MA, Araujo-Neta LSA, Ammirati JF, Baghela A, Bhatt RP, Bojantchev D, Buyck B, Silva GAS, de Lima CLF, de Oliveira RJV, de Souza CAF, Dai YC, Dima B, Duong TTD, Ercole E, Mafalda-Freire F, Ghosh A, Hashimoto A, Kamolhan S, Kang JC, Karunarathna SC, Kirk PM, Kytövuori I, Lantieri A, Liimatainen K, Liu ZY, Liu XZ, Lücking R, Medardi G, Mortimer PE, Nguyen TTTN, Promputtha I, Raj KNA, Reck MA, Lumyong S, Shahzadeh-Fazel SA, Stadler M, Soudi MR, Su HY, Takahashi T, Tangthirasunun N, Uniyal P, Wang Y, Wen TC, Xu JC, Zhang ZK, Zhao YC, Zhou JL, Zhu L (2016) Fungal diversity notes 367–490: taxonomic and phylogenetic contributions to fungal taxa. Fungal Diversity 80: 1–270. https://doi.org/10.1007/s13225-016-0373-x

Hyde KD, Norphanphoun C, Abreu VP, Bazzicalupo A, Thilini Chethana KW, Clericuzio M, Dayarathne MC, Dissanayake AJ, Ekanayaka AH, Zhao RL, Mortimer PE (2017) Fungal diversity notes 603–708: Taxonomic and phylogenetic notes on genera and species. Fungal Diversity 87: 1–235. https://doi.org/10.1007/s13225-017-0391-3

Hyde K, Tennakoon D, Jeewon R, Bhat DJ, Maharachchikumbura S, Rossi W, Leonardi M, Lee H, Mun HY, Houbraken J, Nguyễn T, Jeon S, Frisvad J, Wanasinghe D, Lücking R, Aptroot A, Cáceres M, Karunarathna S, Hongsanan S, Doilom M (2019) Fungal diversity notes 1036–1150: Taxonomic and phylogenetic contributions on genera and species of fungal taxa. Fungal Diversity 96: 1–242. https://doi.org/10.1007/s13225-019-00429-2

Jayasiri SC, Jones EBG, Kang JC, Promputtha I, Bahkali AH, Hyde KD (2016) A new species of genus *Anteaglonium* (Anteagloniaceae, Pleosporales) with its asexual morph. Phytotaxa 263(3): 233–244. https://doi.org/10.11646/phytotaxa.263.3.4

Katoh K, Standley D (2013) MAFFT multiple sequence alignment software version 7: Improvements in performance and usability. Molecular Biology and Evolution 30(4): 772–780. https://doi.org/10.1093/molbev/mst010

Koukol O, Delgado G (2019) Do not forget Africa-revision of fungarium collections at Kew revealed a new species of *Hermatomyces* (Hermatomycetaceae, Pleosporales). Nova Hedwigia 109(3/4): 413–423. https://doi.org/10.1127/nova_hedwigia/2019/0559

Koukol O, Delgado G, Hofmann TA, Piepenbring M (2018) Panama, a hot spot for *Hermatomyces* (Hermatomycetaceae, Pleosporales) with five new species, and a critical synopsis of the genus. IMA Fungus 9(1): 107–141. https://doi.org/10.5598/imafungus.2018.09.01.08

Koukol O, Delgado G, Tabé A, Yorou NS (2025) The genus Hermatomyces in Benin, with the description of *H. griseomarginatus*, sp. nov. Mycologia 117(2): 286–296. https://doi.org/10.1080/00275514.2024.2433367

Leão-Ferreira S, Gusmao L, Castañeda-Ruiz R (2013) Conidial fungi from the semi-arid Caatinga biome of Brazil. Three new species and new records. Nova Hedwigia 96: 479–494. https://doi.org/10.1127/0029-5035/2013/0084

Liu YJ, Whelen S, Hall BD (1999) Phylogenetic relationships among ascomycetes: Evidence from an RNA polymerse II subunit. Molecular Biology and Evolution 16: 1799–1808. https://doi.org/10.1093/oxfordjournals.molbev.a026092

Liu NG, Hyde KD, Sun YR, Bhat DJ, Jones EBG, Jumpathong J, Lin CG, Lu YZ, Yang J, Liu LL, Liu ZY, Liu JK (2024) Notes, outline, taxonomy and phylogeny of brown-spored hyphomycetes. Fungal Diversity 129(1): 1–281. https://doi.org/10.1007/s13225-024-00539-6

Nuankaew S, Suetrong S, Wutikhun T, Pinruan U (2019) *Hermatomyces trangensis* sp. nov., a new dematiaceous hyphomycete (Hermatomycetaceae, Pleosporales) on sugar palm in Thailand. Phytotaxa 391(5): 277–288. https://doi.org/10.11646/phytotaxa.391.5.1

O'Donnell K, Cigelnik E (1997) Two divergent intragenomic rDNA ITS2 types within a monophyletic lineage of the fungus *Fusarium* are nonorthologous. Molecular Phylogenetics and Evolution 7: 103–116. https://doi.org/10.1006/mpev.1996.0376

Phukhamsakda C, McKenzie EHC, Phillips AJL, Gareth Jones EB, Jayarama Bhat D, Stadler M, Bhunjun CS, Wanasinghe DN, Thongbai B, Camporesi E, Ertz D, Jayawardena RS, Perera RH, Ekanayake AH, Tibpromma S, Doilom M, Xu JC, Hyde KD (2020) Microfungi associated with *Clematis* (Ranunculaceae) with an integrated approach to delimiting species boundaries. Fungal Diversity 102: 1–203. https://doi.org/10.1007/s13225-020-00448-4

Rao V, de Hoog GS (1986) New or critical hyphomycetes from India. Studies in Mycology 28: 1–84.

Rehner SA, Buckley E (2005) A Beauveria phylogeny inferred from nuclear ITS and EF1-α sequences: Evidence for cryptic diversification and links to Cordyceps teleomorphs. Mycologia 97: 84–98. https://doi.org/10.1080/15572536.2006.11832842

Ren GC, Wanasinghe DN, Monkai J, Mortimer PE, Hyde KD, Xu JC, Pang A, Gui H (2021) Novel saprobic *Hermatomyces* species (Hermatomycetaceae, Pleosporales) from China (Yunnan Province) and Thailand. MycoKeys 82: 57–79. https://doi.org/10.3897/mycokeys.82.67973

Ren GC, Wanasinghe DN, Jeewon R, Monkai J, Mortimer PE, Hyde KD, Xu JC, Gui H (2022) Taxonomy and phylogeny of the novel *Rhytidhysteron*-like collections in the Greater Mekong Subregion. MycoKeys 86: 65–85. https://doi.org/10.3897/mycokeys.86.70668

Ronquist F, Teslenko M, Van Der Mark P, Ayres DL, Darling A, Höhna S, Larget B, Liu L, Suchard MA, Huelsenbeck JP (2012) MrBayes 3.2: Efficient Bayesian phylogenetic inference and model choice across a large model space. Systematic Biology 61: 539–542. https://doi.org/10.1093/sysbio/sys029

Samuels GJ, Müller E (1979) Life-history studies of Brazilian Ascomycetes. 7. *Rhytidhysteron rufulum* and the genus Eutryblidiella. Sydowia 32: 277–292.

Senanayake IC, Rathnayaka AR, Marasinghe DS, Calabon MS, Gentekaki E, Lee HB, Hurdeal VG, Pem D, Dissanayake LS, Wijesinghe SN, Bundhun D, Nguyen TT, Goonasekara ID, Abeywickrama PD, Bhunjun CS, Jayawardena RS, Wanasinghe DN, Jeewon R, Bhat DJ, Xiang MM (2020) Morphological approaches in studying fungi: Collection,

examination, isolation, sporulation and preservation. Mycosphere: Journal of Fungal Biology 11(1): 2678–2754. https://doi.org/10.5943/mycosphere/11/1/20

Shen HW, Luo ZL, Bao DF, Luan S, Bhat DJ, Boonmee S, Wang WP, Su XJ, Li YX, Al-Otibi F, Lu YZ, Yang LQ, Hyde KD (2024) Lignicolous freshwater fungi from China IV: Morphology and phylogeny reveal new species of Pleosporales from plateau lakes in Yunnan Province, China. Mycosphere: Journal of Fungal Biology 15(1): 6439–6524. https://doi.org/10.5943/mycosphere/15/1/28

Shukla R, Pandey N, Banerjee S, Tripathi YB (2017) Effect of extract of *Pueraria* tuberosa on expression of hypoxia inducible factor-1α and vascular endothelial growth factor in kidney of diabetic rats. Biomedicine & Pharmacotherapy = Biomédecine & Pharmacothérapie 93: 276–285. https://doi.org/10.1016/j.biopha.2017.06.045

Singhal RK (2009) Mining and the environment: From ore to metal. International Journal of Mining, Reclamation and Environment 23(4): e241. https://doi.org/10.1080/17480930903429794

Son E, Yoon JM, An BJ, Lee YM, Cha J, Chi GY, Kim DS (2019) Comparison among activities and isoflavonoids from *Pueraria thunbergiana* aerial parts and root. Molecules 24(5): e912. https://doi.org/10.3390/molecules24050912

Soto-Medina E, Lücking R (2017) A new species of *Rhytidhysteron* (Ascomycota: Patellariaceae) from Colombia, with a provisional working key to known species in the world Artículo original. Revista de la Academia Colombiana de Ciencias Exactas, Físicas y Naturales 41(158): 59–63. https://doi.org/10.18257/raccefyn.423

Spegazzini C (1881) Fungi argentini additis nonnullis brasiliensibus montevideensibusque. Pugillus quartus (Continuacion). Anales de la Sociedad Científica Argentina 12: 174–189.

Spegazzini C (1910) Mycetes argentinenses (Series V). Anales del Museo Nacional de Historia Natural Buenos Aires 20: 329–467.

Sun R, Deng X, Zhang D, Xie F, Wang D, Wang J, Tavallaie MS, Jiang F, Fu L (2019) Anti-diabetic potential of *Pueraria lobata* root extract through promoting insulin signaling by PTP1B inhibition. Bioorganic Chemistry 87: 12–15. https://doi.org/10.1016/j.bioorg.2019.02.046

Thambugala KM, Hyde KD, Eungwanichayapant PD, Romero AI, Liu ZY (2016) Additions to the genus *Rhytidhysteron* in Hysteriaceae. Cryptogamie. Mycologie 37(1): 99–116. https://doi.org/10.7872/crym/v37.iss1.2016.99

Tibpromma S, Bhat DJ, Doilom M, Lumyong S, Nontachaiyapoom S, Yang JB, Hyde KD (2016) Three new *Hermatomyces* species (Lophiotremataceae) on *Pandanus odorifer* from Southern Thailand. Phytotaxa 275(2): 127–139. https://doi.org/10.11646/phytotaxa.275.2.4

Tibpromma S, Hyde KD, Jeewon R, Maharachchikumbura SSN, Liu JK, Bhat DJ, Jones EBG, McKenzie EHC, Nontachaiyapoom S, Wen TC, Karunarathna SC (2017) Fungal diversity notes 491–602: Taxonomic and phylogenetic contributions to fungal taxa. Fungal Diversity 83: 1–261. https://doi.org/10.1007/s13225-017-0378-0

Tibpromma S, Hyde KD, McKenzie EHC, Bhat DJ, Phillips AJL, Wanasinghe DN, Samarakoon MC, Jayawardena RS, Dissanayake AJ, Tennakoon DS, Doilom M, Phookamsak R, Tang AMC, Xu JC, Mortimer PE, Promputtha I, Maharachchikumbura SSN, Khan S, Karunarathna SC (2018) Fungal diversity notes 840–928: Micro-fungi associated with Pandanaceae. Fungal Diversity 93: 1–160. https://doi.org/10.1007/s13225-018-0408-6

Vilgalys R, Hester M (1990) Rapid genetic identification and mapping of enzymatically amplified ribosomal DNA from several *Cryptococcus* species. Journal of Bacteriology 172: 4238–4246. https://doi.org/10.1128/jb.172.8.4238-4246.1990

Wanasinghe DN, Mortimer PE, Xu J (2021) Insight into the systematics of microfungi colonizing dead woody twigs of *Dodonaea viscosa* in Honghe (China). Journal of Fungi 7(3): e180. https://doi.org/10.3390/jof7030180

Wang XL, Jiao FR, Yu M, Lin LB, Xiao J, Zhang Q, Wang L, Duan DZ, Xie G (2017) Constituents with potent α-glucosidase inhibitory activity from *Pueraria lobata* (Willd.) ohwi. Bioorganic & Medicinal Chemistry Letters 27(9): 1993–1998. https://doi.org/10.1016/j.bmcl.2017.03.013

Wang S, Zhang S, Wang S, Gao P, Dai L (2020) A comprehensive review on *pueraria*: Insights on its chemistry and medicinal value. Biomedicine & Pharmacotherapy = Biomédecine & Pharmacothérapie 131: e110734. https://doi.org/10.1016/j.biopha.2020.110734

Wang HX, Zeng MS, Ye Y, Liu JY, Xu PP (2021) Antiviral activity of *puerarin* as potent inhibitor of influenza virus neuraminidase. Phytotherapy Research: PTR 35(1): 324–336. https://doi.org/10.1002/ptr.6803

White T, Bruns T, Lee S, Taylor J (1990) Amplification and direct sequencing of fungal ribosomal RNA genes for phylogenetics. PCR Protocols: A Guide to Methods and Applications 18: 315–322. https://doi.org/10.1016/B978-0-12-372180-8.50042-1

Wijayawardene NN, Phillips AJL, Tibpromma S, Dai DQ, Selbmann L, Monteiro JS, Aptroot A, Flakus A, Rajeshkumar KC, Coleine C, Pereira DS, Fan X, Zhang L, Maharachchikumbura SSN, Souza MF, Kukwa M, Suwannarach N, Rodriguez-Flakus P, Ashtekar N, Dauner L, Tang LZ, Jin XC, Karunarathna SC (2021) Looking for the undiscovered asexual taxa: Case studies from lesser studied life modes and habitats. Mycosphere: Journal of Fungal Biology 12(1): 1290–1333. https://doi.org/10.5943/mycosphere/12/1/17

Xiong Y, Yang Y, Yang J, Chai H, Li Y, Yang J, Jia Z, Wang Z (2010) Tectoridin, an isoflavone glycoside from the flower of *Pueraria lobata*, prevents acute ethanol-induced liver steatosis in mice. Toxicology 276(1): 64–72. https://doi.org/10.1016/j.tox.2010.07.007

Xu L, Zheng N, He Q, Li R, Zhang K, Liang T (2013) Puerarin, isolated from *Pueraria lobata* (Willd.), protects against hepatotoxicity via specific inhibition of the TGFbeta1/Smad signaling pathway, thereby leading to anti-fibrotic effect. Phytomedicine: International Journal of Phytotherapy and Phytopharmacology 20(13): 1172–1179. https://doi.org/10.1016/j.phymed.2013.06.008

Yang YY, Li TS, Bhunjun CS, Thiyagaraja V, Bhat DJ, He SC, Zhao Q, Al-Otibi F, Kakumyan P, Hyde KD (2025) Two novel species of *Hermatomyces* (Dothideomycetes) from Fagales in China. Mycological Progress. https://doi.org/10.1007/s11557-025-02105-z

Zhang B, Li W, Dong M (2017) Flavonoids of kudzu root fermented by eurtotium cristatum protected rat pheochromocytoma line 12 (PC12) cells against H_2O_2-Induced apoptosis. International Journal of Molecular Sciences 18(12): e2754. https://doi.org/10.3390/ijms18122754

Zhang L, Fang DY, Liu C, Zhao DY, Wang YJ, Chen WN, Cui Y, Guo JF, Cong PW, Feng XF, Zhang YT (2021) Mechanism of puerarin reversing SH-SY5Y cell injury induced by Aβ_(1-42) based on proteomics. Zhongguo Zhongyao Zazhi 46(14): 3650–3659. https://doi.org/10.19540/j.cnki.cjcmm.20210201.403

Zhang YZ, Chen Q, Ma J, Lu YZ, Chen H, Liu NG (2023) Morphological and multi-gene phylogenetic analyses reveal five new hyphomycetes from freshwater habitats. Frontiers in Microbiology 14: e1253239. https://doi.org/10.3389/fmicb.2023.1253239